

Supplementary Materials for

PSMA-Targeted Contrast Agents for Intraoperative Imaging of Prostate Cancer

Kai Bao^{1,2}, Jeong Heon Lee¹, Homan Kang¹, G. Kate Park¹, Georges El Fakhri¹,
and Hak Soo Choi^{1**}

¹Gordon Center for Medical Imaging, Department of Radiology, Massachusetts General Hospital
and Harvard Medical School, Boston, MA 02114, USA

² Key Laboratory of Structure-Based Drug Design & Discovery, Ministry of Education,
Shenyang Pharmaceutical University, Shenyang 110016, China.

****Correspondence** to H.S.C. @ hchoi12@mgh.harvard.edu

The PDF file includes:

Supplementary Methods

Figure S1. Physicochemical properties of PEG-linked KUE conjugates.

Figure S2. UPLC and MALDI analysis of KUE-PEG_x-ZW800-1 (x = 2, 4, 12, 24).

Figure S3. UPLC analysis and ESI-TOF (+) mass spectrum of PEG₄-linked KUE conjugates.

Figure S4. UPLC analysis and ESI-TOF (+) mass spectrum of PEG_x-linked KUE-ZW800+3C conjugates (x = 0, 2, 4, 12, 24).

Figure S5. *In vitro* PSMA targeting assay of KUE-PEG₄-linked NIR fluorophores and KUE-PEG_x-linked ZW800+3C conjugates (x = 0, 2, 4, 12, or 24).

Figure S6. *In vivo* biodistribution of ZW800+3C and KUE-PEG₄-ZW800+3C in mice.

Supplementary Methods

Reagents: Unless otherwise noted, all the materials were American Chemical Society grade or higher, and obtained from commercially available sources and were used without purification. HPLC-grade solvents were purchased from Fisher Scientific (Pittsburgh, PA) and Sigma-Aldrich (Saint Louis, MO). Ultra dry DMSO was purchased from Acros Organics (Geel, Belgium). Cy5.5 and Cy7 were purchased from GE Healthcare (Piscataway, NJ), while ZW800-1, ZW800-3C, and ZW800+3C were synthesized as previously reported.¹⁻³

KUE conjugation: Generally, the synthesis of the KUE-fluorophores involved one or two times activation of the carboxyl group for the subsequent conjugation. In our case, dipyrrolidino(N-succinimidyl)carbenium hexafluorophosphate (HSPyU) was utilized to generate the NHS ester forms of the NIR fluorophores in the presence of diisopropylethylamine (DIEA) in dimethyl sulfoxide (DMSO). The separation and purification of the NHS ester were performed smoothly by using simple precipitations in different solvents system, without the chromatographic process. The conjugation of KUE and PEG spacer with the NIR fluorophores had minimal impact on the spectral properties of each NIR fluorophore.

HPLC purification: HPLC purification of compounds was performed on a Waters (Milford, MA) prepHPLC 150 mL fluid handling unit equipped with a symmetry Prep C18 column (19 x 150 mm, 7 μ m particle size), a dual-wavelength absorbance detector (254 and 700 nm), a manual injector (Rheodyne 3725i) and a 2487 dual wavelength absorbance detector outfitted with a semi-preparative flow cell. Solvent A was water with 0.1% formic acid and solvent B was absolute methanol 0.1% formic acid. The purification utilized a linear gradient from 10% to 90% solvent B over 30 min. Mobile phase flow rate was 15 mL/min.

ES-TOF mass spectroscopic analysis: The purity of all compounds was measured using ultra-performance liquid chromatography (UPLC, Waters) combined with simultaneous ELSD,

absorbance (photodiode array), fluorescence and electrospray time-of-flight (ES-TOF) mass spectrometry (MS). UPLC analyses were carried out using a Waters ACQUITY UPLC HSS C18 column (2.1x50 mm, 1.8 μ m) and Xevo G2 QToF detector connected to a PC with a MassLynx 4.1 workstation. The mobile phase was solvent A = 0.1% formic acid in water, solvent B = 0.1% formic acid in methanol with a linear gradient from 10% to 90% (from A to B for 5 minutes). The flow rate was 0.6 mL/min and all compounds were identified by mass to charge ratio.

Physicochemical and optical property analyses: The partition coefficient (logD at pH 7.4), topological polar surface area (TPSA), and net charges of each fluorescent conjugate were calculated using JChem Calculator plugins (ChemAxon, Budapest, Hungary). All optical measurements were performed at 37°C in 100% fetal bovine serum (FBS) buffered with 50 mM HEPES, pH 7.4. Absorbance and fluorescence spectra for all fluorescent conjugates were collected using online fiberoptic HR2000 absorbance (200-1100 nm) and USB2000FL fluorescence (350-1,000 nm) spectrometers (Ocean Optics, Dunedin, FL). Excitation light was provided by a 5 mW of 650 nm red laser pointer (Opcom Inc., Xiamen, China) and 8 mW of 765 nm NIR laser diode light source (Electro Optical Components, Santa Rosa, CA) coupled through a 300 μ m core diameter, NA 0.22 fiber (Fiberguide Industries, Stirling, NJ). *In silico* calculations of the partition coefficient (logD at pH 7.4), 2D and 3D stabilized structures were calculated using JChem calculator plugins (ChemAxon, Budapest, Hungary). The 3D conformer of bioconjugates was calculated by using MarvinSketch 16.12.12 software (ChemAxon) to generate bioactive ligand geometries in minimally sized conformer sets.

***In vitro* PSMA targeting assay:** Human prostate cancer cells (PC-3 and LNCaP) were purchased from the ATCC (Manassas, VA). The cells lines were cultured at 37 °C, in a humidified atmosphere containing 5% CO₂, in RPMI 1640 medium (Mediatech Cellgro) supplemented with 10% of fetal bovine serum (Gemini Biotech Products, Woodland, CA) and 5% of penicillin/streptomycin (Cambrex Bio Science, Walkersville, MD). Exponentially growing

LNCaP and PC-3 cells at a confluence of 75% on glass coverslips were incubated for 60 min at 4 °C with 0.2 mL of TBS containing 2 μ M of each fluorophore. The cells were washed three times with TBS, and imaged on a previously described four-channel NIR fluorescence microscope.

***In vivo* biodistribution and clearance:** Animals were housed in an AAALAC-certified facility and were studied under the supervision of BIDMC IACUC in accordance with the approved institutional protocol (#057-2014). Male CD-1 mice weighing roughly 20 g were purchased from Charles River Laboratories (Wilmington, MA) and male NCr nu/nu mice 5 to 6 weeks of age weighing 22 g \pm 3 g were purchased from Taconic Farms (Germantown, NY). Animals were anesthetized with 100 mg/kg ketamine and 10 mg/kg xylazine intraperitoneally (Webster Veterinary, Fort Devens, MA). 10-25 nmol (0.4-1.0 mg/kg) of the NIR fluorophore conjugate in saline were administered intravenously, and animals were imaged with our real-time intraoperative imaging system.⁴⁻¹⁰ In this study, 670 nm excitation and 760 nm excitation fluence rates used were 4.0 and 11.0 mW/cm², respectively, with white light (400 to 650 nm) at 40,000 lx. Color video and 2 independent channels (700 nm and 800 nm) of NIR fluorescence images were acquired simultaneously with custom FLARE software at rates up to 15 Hz over a 15 cm diameter field of view (FOV). The imaging system was positioned at a distance of 18 inches from the surgical field. A custom filter set (Chroma Technology Corporation, Brattleboro, VT) composed of a 750 \pm 25 nm excitation filter, a 785 nm dichroic mirror, and an 810 \pm 20 nm emission filter were used to detect 800 nm fluorophores. For Cy5.5 detection, we used 650 \pm 22 nm and 710 \pm 25 nm excitation and emission filters. For each experiment, camera exposure time and image normalization was held constant. To quantify the blood clearance rate and urinary excretion, intermittent sampling from the tail vein was performed over the 4 h period following intravenous administration. Approximately 10-20 μ L of blood were collected using glass capillary tubes at the following time points: 0, 1, 2, 5, 10, 15, 30, 60, 90, 120, 180, and 240 min. Custom intraoperative fluorescence imaging system was used to measure the fluorescence intensity of each sample, and the concentration was calculated based on the image SBR using a

standard curve for each fluorophore. To measure total body excretion in mice, animals were sacrificed at 30, and 240 min, and major tissues and organs were resected and imaged. Using capillary tubes, the amount of NIR fluorophore in each organ/tissue was quantified by measuring fluorescent intensity (photons/s/cm²/sr).

H&E histology and NIR fluorescence microscopy: Resected tumor tissues were placed in 2% paraformaldehyde solutions in phosphate-buffered saline (PBS) for 30 minutes before mounting in Tissue-Tek OCT compound (Fisher Scientific, Pittsburgh, PA) and flash-freezing in liquid nitrogen. Frozen samples were cryosectioned (10 μ m per slice), analyzed by NIR fluorescence microscopy, and also stained with hematoxylin and eosin (H&E). NIR fluorescence microscopy was performed on a 4-filter Nikon Eclipse TE300 microscope system as previously described.^{31, 41} Images were acquired on an Orca-AG apparatus (Hamamatsu, Bridgewater, NJ). Image acquisition and analysis was performed using iVision software (BioVision Technologies, Exton, PA). Custom filter set (Chroma Technology Corporation, Brattleboro, VT) with 750 \pm 25 nm excitation filters, 785 nm dichroic mirrors, and 810 \pm 20 nm emission filters were used to detect imaging signals in the frozen tissue samples.

Quantitative analysis: At each time point, the fluorescence and background intensity of a region of interest (ROI) over each tissue was quantified using custom imaging software and ImageJ v1.48 (NIH, Bethesda, MD). The signal-to-background ratio (SBR) was calculated as $SBR = \text{fluorescence}/\text{background}$, where background is the signal intensity of neighbouring tissues such as muscle or skin obtained over the period of imaging time. All NIR fluorescence images for a particular fluorophore were normalized identically for all conditions of an experiment. At least three animals were analysed at each time point. Statistical analysis was carried out using the unpaired Student's t-test or one-way analysis of variance (ANOVA). Results are presented as mean standard deviation, and curve fitting was performed using the Prism version 4.0a software (GraphPad, San Diego, CA).

A.			
PEG linker	MW (Da)	Atoms	Length (Å)
Amino-dPEG2-acid	177.10	10	10.9
Amino-dPEG4-acid	265.15	16	18
Amino-dPEG12-acid	617.36	40	46.5
Amino-dPEG24-acid	1145.68	76	89

B.			
KUE conjugate	MW (Da)	LogD, pH 7.4	TPSA (Å)
KUE-ZW800-1A	1246.58	-7.75	312.01
KUE-PEG2-ZW800-1	1405.67	-8.71	359.57
KUE-PEG4-ZW800-1	1493.72	-8.80	365.97
KUE-PEG12-ZW800-1	1845.93	-9.18	451.87
KUE-PEG24-ZW800-1	2374.24	-9.74	562.63

C.			
KUE conjugate	MW (Da)	LogD, pH 7.4	TPSA (Å)
KUE-ZW800+3C	1302.40	-9.00	401.50
KUE-PEG2-ZW800+3C	1460.48	-9.96	449.06
KUE-PEG4-ZW800+3C	1549.54	-13.65	483.20
KUE-PEG12-ZW800+3C	1901.75	-10.43	541.36
KUE-PEG24-ZW800+3C	2430.06	-11.00	652.12

Figure S1. Physicochemical properties of PEG-linked KUE conjugates. Polar surface area and hydrophobicity distributions were depicted using MarvinSketch 6.2.2 (ChemAxon). Log*D* = partition coefficient; TPSA = topological polar surface area.

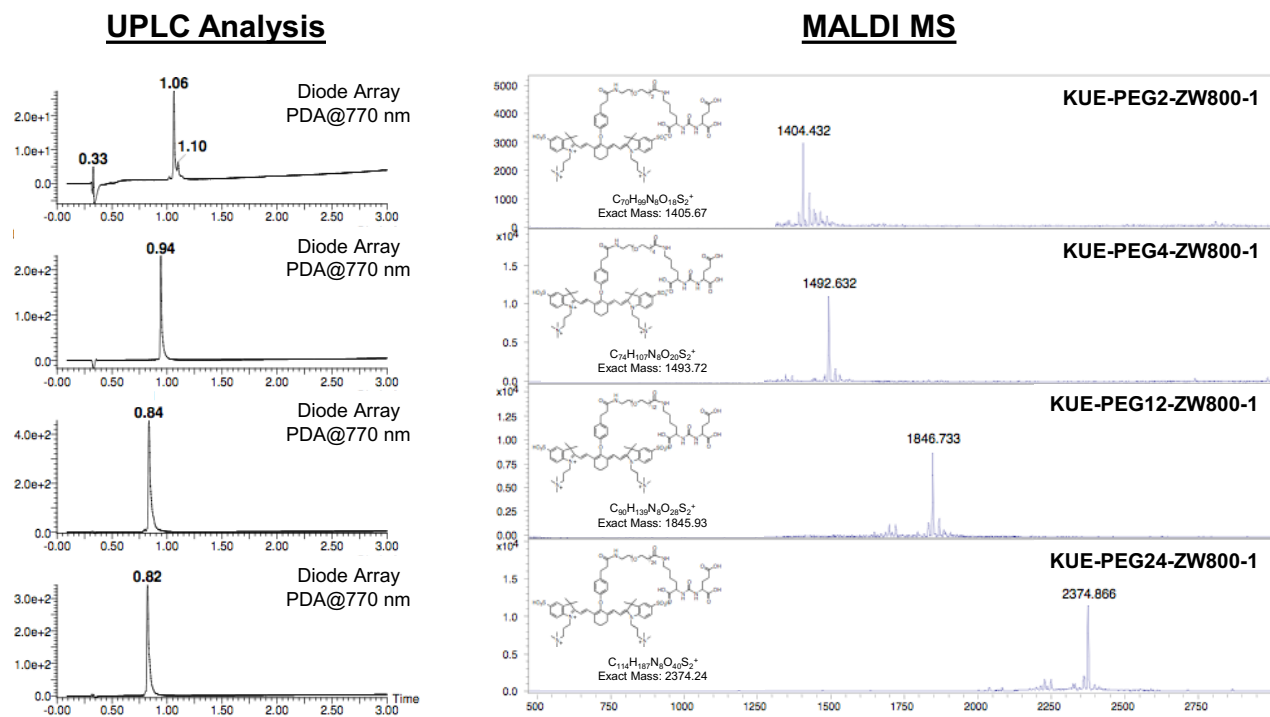


Figure S2. UPLC and MALDI analysis of KUE-PEG_x-ZW800-1 (x= 2, 4, 12, 24).

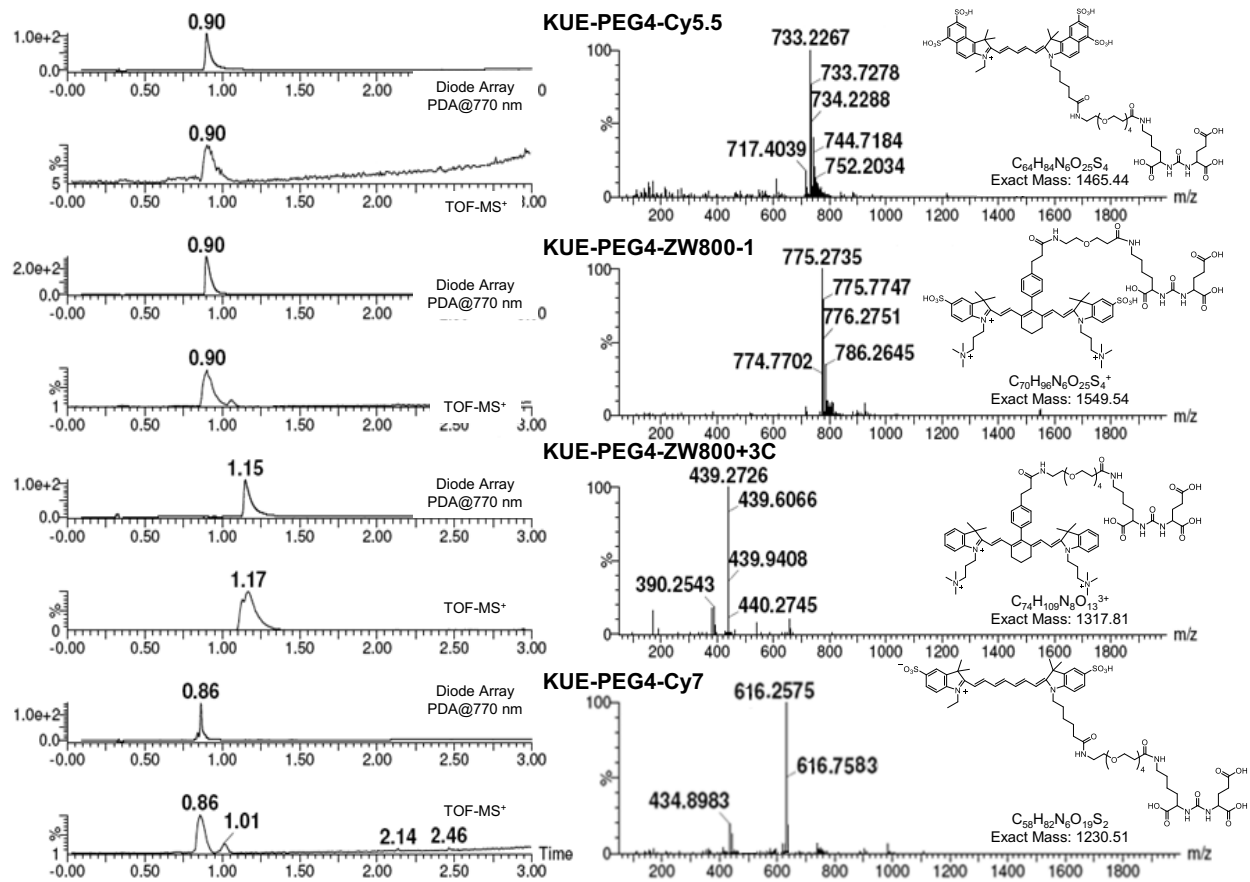


Figure S3. UPLC analysis and ESI-TOF mass spectrum (+) of PEG4-linked KUE conjugates.

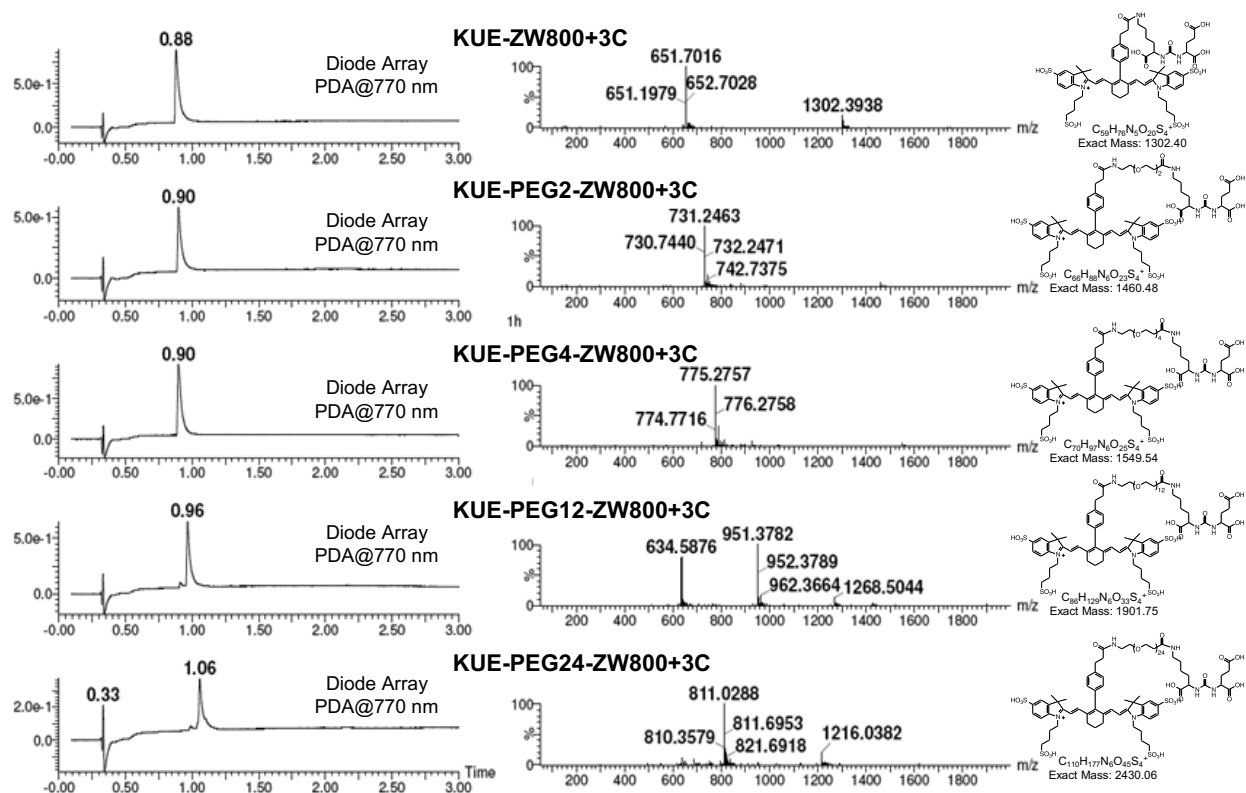


Figure S4. UPLC analysis and ESI-TOF (+) mass spectrum of PEG_x-linked KUE-ZW800+3C conjugates (x = 0, 2, 4, 12, 24).

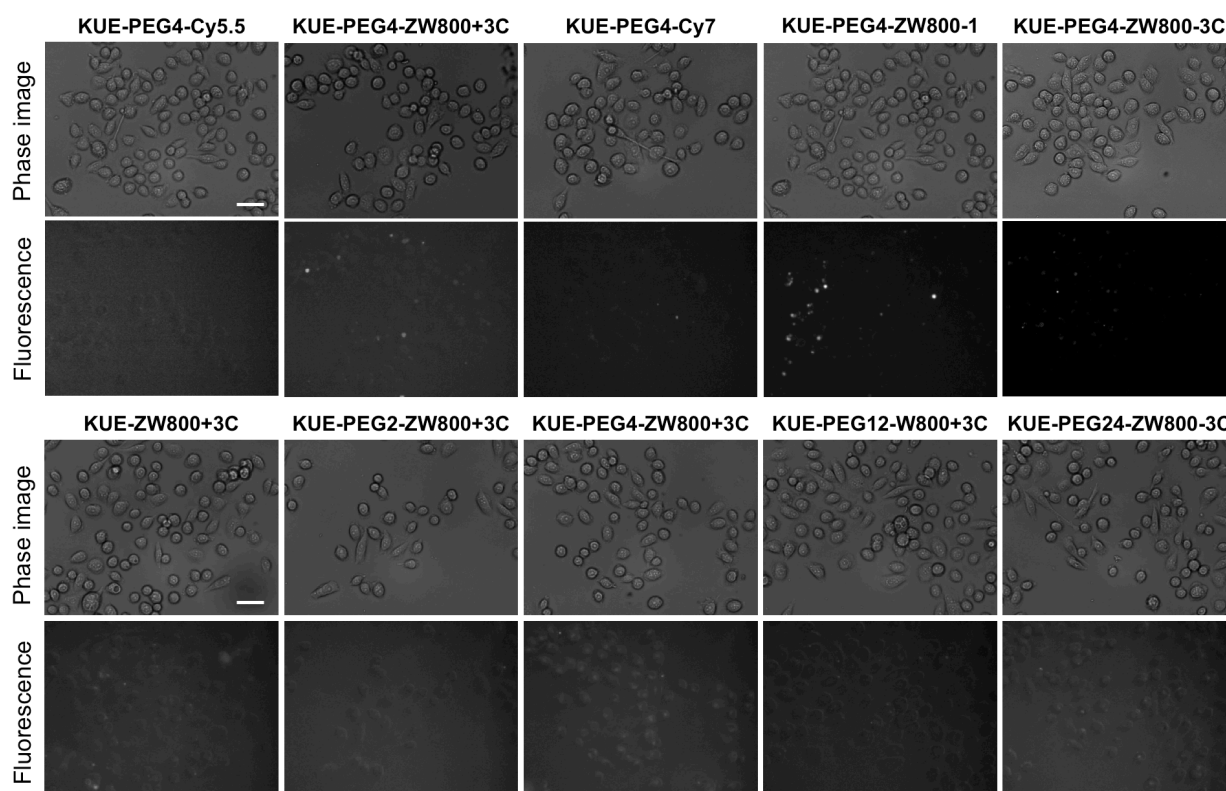


Figure S5. *In vitro* PSMA targeting assay on living prostate cancer cells: A series of (a) KUE-PEG4-linked NIR fluorophores and (b) KUE-PEG_x-linked ZW800+3C conjugates (x = 0, 2, 4, 12, or 24) were incubated at a concentration of 2 μ M in PSMA-negative PC3 cells at 4 $^{\circ}$ C for 60 min prior to washing and image acquisition. Fluorescence images have identical exposure time and normalization. Scale bars = 100 μ m.

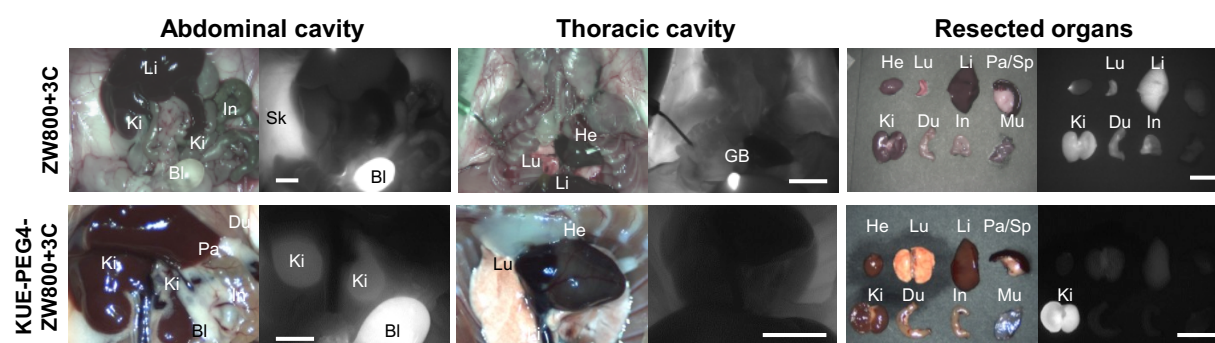


Figure S6. *In vivo* biodistribution of ZW800+3C and KUE-PEG4-ZW800+3C in mice. Each NIR fluorophore was intravenously injected into 20 g CD-1 mice (10 nmol; 0.4 mg/kg) 4 h prior to imaging. Images are representative of n = 3 independent experiments. Abbreviations used are: Bl, bladder; Du, duodenum; He, heart; In, intestine; Ki, kidney; Li, liver; Lu, lung; Mu, muscle; Pa, pancreas; Sp, spleen. Scale bars = 1 cm.

References

1. H. S. Choi, S. L. Gibbs, J. H. Lee, S. H. Kim, Y. Ashitate, F. Liu, H. Hyun, G. Park, Y. Xie, S. Bae, M. Henary and J. V. Frangioni, *Nat Biotechnol*, 2013, **31**, 148-153.
2. H. Hyun, M. W. Bordo, K. Nasr, D. Feith, J. H. Lee, S. H. Kim, Y. Ashitate, L. A. Moffitt, M. Rosenberg, M. Henary, H. S. Choi and J. V. Frangioni, *Contrast Media Mol Imaging*, 2012, **7**, 516-524.
3. H. Hyun, E. A. Owens, L. Narayana, H. Wada, J. Gravier, K. Bao, J. V. Frangioni, H. S. Choi and M. Henary, *RSC Adv*, 2014, **4**, 58762-58768.
4. H. S. Choi, W. Liu, P. Misra, E. Tanaka, J. P. Zimmer, B. Itty Ipe, M. G. Bawendi and J. V. Frangioni, *Nat Biotechnol*, 2007, **25**, 1165-1170.
5. H. S. Choi, B. I. Ipe, P. Misra, J. H. Lee, M. G. Bawendi and J. V. Frangioni, *Nano Lett*, 2009, **9**, 2354-2359.
6. H. S. Choi, Y. Ashitate, J. H. Lee, S. H. Kim, A. Matsui, N. Insin, M. G. Bawendi, M. Semmler-Behnke, J. V. Frangioni and A. Tsuda, *Nat Biotechnol*, 2010, **28**, 1300-1303.
7. H. Hyun, M. Henary, T. Gao, L. Narayana, E. A. Owens, J. H. Lee, G. Park, H. Wada, Y. Ashitate, J. V. Frangioni and H. S. Choi, *Mol Imaging Biol*, 2016, **18**, 52-61.
8. H. Hyun, E. A. Owens, H. Wada, A. Levitz, G. Park, M. H. Park, J. V. Frangioni, M. Henary and H. S. Choi, *Angew Chem Int Ed Engl*, 2015, **54**, 8648-8652.
9. H. Hyun, M. H. Park, E. A. Owens, H. Wada, M. Henary, H. J. Handgraaf, A. L. Vahrmeijer, J. V. Frangioni and H. S. Choi, *Nat Med*, 2015, **21**, 192-197.
10. H. Hyun, H. Wada, K. Bao, J. Gravier, Y. Yadav, M. Laramie, M. Henary, J. V. Frangioni and H. S. Choi, *Angew Chem Int Ed Engl*, 2014, **53**, 10668-10672.